Mechanism of Macroion−Macroion Clustering Induced by the Presence of Trivalent Counterions

E. Spohr[†]

Department of Theoretical Chemistry, University of Ulm, D-89069 Ulm, Germany

B. Hribar and V. Vlachy*

Faculty of Chemistry and Chemical Technology, University of Ljubljana, 1000 Ljubljana, Slovenia

Received: October 15, 2001

The results of molecular dynamics simulations for a soft sphere model of highly asymmetric electrolyte solutions containing macroions and counterions are presented. The macroions carry a negative charge of 12 or 24 elementary charges and the solutions contain monovalent, divalent or trivalent ($z_c = +1$, $+2$, or $+3$) counterions. The size ratio between macroion and counterion was chosen to be about 5:1 and 7:1. From analysis of both static and dynamic properties we propose a mechanism for the observed formation of clusters between equally charged macroions in these solutions.

1. Introduction

Aqueous solutions of charged colloids, surfactant micelles, and polyelectrolytes play an important role in our everyday life. Experimental evidence suggests that charged macroions are stabilized by electrostatic forces, and it is usually assumed that the Deryaguin−Landau−Verwey−Overbeek (DLVO) theory[1,2] is applicable to these systems. In this theory the interaction potential acting between a pair of macroions is written as the sum of the repulsive screened Coulomb potential and the attractive van der Waals interaction. Accordingly, in the absence of van der Waals forces the interaction potential between equally charged macroions can only be repulsive. The theoretical and some experimental studies performed in the last 25 years (for reviews see refs 3−7), indicate that strong interactions between macroions and counterions lead to instability, which is not accounted for by the classical DLVO theory. While there is considerable experimental evidence of electrostatic attraction between cylindrical particles surrounded with multivalent counterions,[8−11] direct evidence of such an interaction between spherical macroions has only been presented recently.[12] The large number of papers published in the past few years[13−32] reflect interest in the nature of macroion−macroion interactions in polyelectrolyte solutions and the importance of this subject for science and technology.

In previous papers[13,19] we published Monte Carlo results for solutions of highly asymmetric electrolytes where macroions, possessing a charge of 20 or 12 negative elementary charges, were neutralized with monovalent ($z_c = +1$), divalent ($z_c = +2$), or trivalent ($z_c = +3$) counterions. The numerical results indicated that the valency of the counterions plays an important role in determining the structural and thermodynamic properties of these solutions. For example, when monovalent counterions are replaced by divalent ones,[13] the macroions approach each other; and in the case of trivalent counterions, the probability of finding two macroions at contact is highest.[19] These data are clearly inconsistent with the classical DLVO theory.[2] In subsequent studies solutions where mixtures of mono- and divalent (or mono- and trivalent) counterions were examined,[20,29] it was demonstrated that the structure of the solution, as reflected in the macroion−macroion pair distribution functions, gradually changes from repulsive in solutions with only monovalent couterions to attractive in solutions where trivalent counterions are present in excess. The effects of addition of simple salts or a neutral component to solutions with divalent and trivalent counterions were also evaluated.[21,22]

Solutions with higher asymmetry in size and charge (60 elementary charges on a macroion) were examined by Linse and co-workers.[16,23,24,30,31] In particular, Linse and Reščič[24,30] studied a model system of highly charged spherical macroions and point counterions by means of Monte Carlo simulations. The effects on the structure of varying the counterion and macroion charge, the dielectric constant of solution, and the macroion concentration were examined. The conclusion of these studies was that at higher electrostatic coupling the system becomes unstable and eventually separates into two phases. The binodal curve was determined and the critical point was estimated.[30]

Despite considerable progress in this area of research, the actual mechanism of cluster formation is still not well understood. So by far most of the information about the structure and thermodynamics of these systems came from Monte Carlo simulations. In the present work we decided to study solutions of highly asymmetric electrolytes by the molecular dynamics (MD) method. In addition to structural properties, which can also be obtained from Monte Carlo simulations, MD simulations can also provide information about the dynamics of the particles in solution. Another difference from our previous studies[13,19] is that the ions are modeled as soft and not as (charged) hard spheres. Such systems of macroions and counterions with a charge ratio -12:$+1$ ($+2$, or $+3$) and -24:$+1$ ($+2$, or $+3$) were studied at two different macroion concentrations, i.e., for $c_m = 0.001$ and 0.005 mol/dm^3.

The paper proceeds as follows: in the next section entitled Model and Methods we will briefly describe the interaction

[†] Current address: Research Center Jülich, IWV-3, D-52425 Jülich, Germany.

10.1021/jp013811d CCC: $22.00
Published on Web 02/09/2002

TABLE 1: Potential Parameters of the Short-Range Potential[a]

set	pair	a/Å	b/Å	σ/Å	$\epsilon/10^{-23}$ J
I	big−big	10.0	10.0	4.0	0.0005
I	big−small	10.0	1.0	4.0	0.01
I	small−small	1.0	1.0	4.0	1.0
II	big−big	15.9	15.9	4.0	0.000333
II	big−small	15.9	1	4.0	0.008
II	small−small	1	1	4.0	1.0

[a] The macroion charge is −12e for set I and −24e for set II.

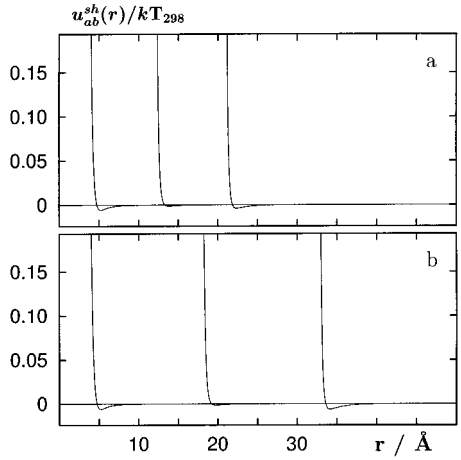

Figure 1. Short-range part of the pair potential u^{sh}/k_BT, $T = 298$ K, for parameter set I (a) and II (b) in Table 1. The curves from left to right are for counterion−counterion, macroion−counterion and macroion−macroion interactions.

model and the simulation methodology before we turn to the analysis of the data (see Results). The paper concludes with a Discussion.

2. Model and Methods

In the present calculation the interaction potential between two particles of species i and j is given by

$$u_{ab}(r) = u_{ab}^{sh}(r) + \frac{e^2 z_a z_b}{4\pi\epsilon_0\epsilon_r r} \quad (1)$$

Here r is the distance between the particles, z_a is the valency of an ion of type a, and e is the proton charge. The indices a and b stand for macroions (m) and counterions (c). The corresponding valencies were $z_m = -12$ (set I of parameters in Table 1) or −24 (set II), and $z_c = +1$, $z_c = +2$, or $z_c = +3$. As usual, the solvent is considered as a continuum with a dielectric constant, ϵ_r, equal to that of bulk water at $T = 298$ K ($\epsilon_r = 78.5$).

The term $u_{ab}^{sh}(r)$ in eq 1 is a short-range potential for composite spheres as proposed by Henderson and Chan.[33] Their rather complicated expression, which will not be repeated here, was obtained from the integral of the Lennard-Jones potential over the two spheres of radius a and b. The two spheres were considered to be filled by a homogeneous distribution of Lennard-Jones sites with parameters ϵ and σ. In the calculation we considered the two sets of parameters presented in Table 1. The short-range potential functions $u_{ab}^{sh}(r)$ are shown in Figure 1. In this figure the counterion−counterion, counterion-macroion, and macroion−macroion short-range potentials are shown from left to right. The effective radius of the particles is usually determined by the balance between Coulomb and short-range interactions. However, a convenient measure for the radius of the particles is the distance at which the short-range potential crosses zero. On the basis of this measure, the counterion radius is 2.4 Å in both parameter sets I and II. The radii of the macroions are 10.9 in parameter set I and 16.8 Å in parameter set II. Note that with these values the macroions described by the second set of parameters (II) possess a smaller surface charge density compared to the macroions described by set I.

Most of the results presented here were obtained by standard molecular dynamics (MD) simulations in the microcanonical ensemble. The MD simulations were carried out at room temperature for systems consisting of 64 macroions and the equivalent number of mono-, di-, and trivalent counterions. The mass of the particles was set arbitrarily to 20 and 200 amu for the small and large spheres, respectively. Constant temperature was maintained through a Berendsen thermostat[34] with a time constant of 5 ps and Newton's equations of motion were integrated with a time step of 0.01 ps. Data acquisition was performed over periods between 5 and 10 ns. In several cases the MD simulation data were supplemented by the Monte Carlo results. The Monte Carlo simulations were performed for the canonical ensemble (at constant volume and temperature) with 64 (or in some cases 128) macroions and an appropriate number of counterions to ensure electroneutrality. Averages were taken over 50−70 million configurations with at least 5 million configurations spent for the equilibration. In all cases (MD and Monte Carlo simulations), the Ewald summation method[35] was used to account for the effects of a finite number of particles. More details concerning the Monte Carlo method are given in our previous papers.[13,19] We note in passing that computer simulations do not contain the usual statistical-mechanical approximations. In this way the results presented here are free of assumptions inherent to the ad-hoc theories designed to explain deviations from the DLVO theory.

3. Results

3.1. Pair Distribution Functions. We begin the discussion by considering the structural features as reflected in the pair distribution functions. In Figure 2 we show the macroion−macroion (g_{mm}), macroion−counterion (g_{mc}), and counterion counterion (g_{cc}) pair distribution functions (pdfs) for the −12:+1 electrolyte solution at macroion concentration $c_m = 0.001$ mol/dm^3. Symbols represent the MC data, while lines connect the MD results. Agreement between the two sets of calculations obtained for the same potential function (eq 1) is very good. The same is true for the −12:+3 electrolyte solution, shown in Figure 3; the value of the $g_{mc}(r)$ peak (off scale) is 485. For solutions with trivalent counterions ($z_c = +3$), the shape of the macroion−macroion pdf indicates an effective attractive interaction between the like-charged macroions. We may therefore conclude that the MD and Monte Carlo results for the charged soft spheres confirm our earlier Monte Carlo calculations performed for the primitive model (charged hard spheres).[19]

Figure 4 presents the macroion−macroion pdfs in solutions with the mono-, di-, and trivalent counterions at $c_m = 0.005$ mol/dm^3 and for $z_m = -12$ (top), and $z_m = -24$ (bottom). The results clearly show pronounced maxima for the −24:+3 and −12:+3 electrolytes, which are absent in the cases where the counterions carry a smaller charge.

3.2. Cluster Analysis. To investigate the process of macroion cluster formation in more detail, we first performed an analysis of macroion−counterion association. For this purpose we defined a "shell" (spherical domain) around a given macroion: a counterion belongs to the particular macroion if it is found to be within a shell, i.e., within a distance of r_c ($r_c = 20$ Å) from

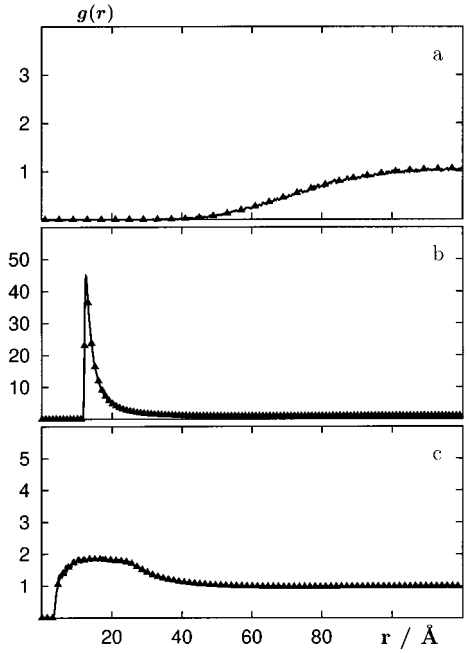

Figure 2. Macroion−macroion (a), macroion−counterion (b), and counterion−counterion (c) pair distribution function for a −12:+1 electrolyte, $c_m = 0.001$ mol dm^{-3}. Lines are for the molecular dynamics results and points are from Monte Carlo calculations.

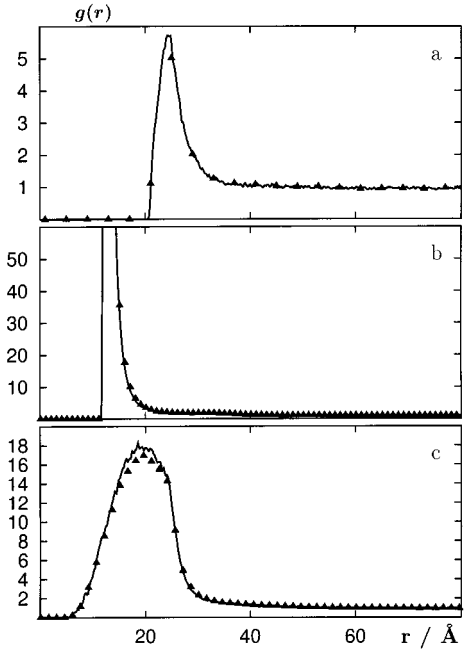

Figure 3. Same as for Figure 2, but for a −12:+3 electrolyte solution.

the macroion center. This somewhat arbitrary value was chosen on the basis of the macroion−counterion distributions. While the pdf itself does not exhibit a well pronounced minimum, the number of counterions in a spherical shell around a macroion, $\rho_c(r)4\pi r^2\,dr$, exhibits a clear minimum in the range from 20 to 25 Å (for model I). We thus chose a rather strict definition. Note that a counterion can belong to more than just one macroion; in other words, it may participate in several "shells".

Figure 5a shows the probability distribution of the number of counterions N_c within shells around macroions for model I at $c_m = 0.005$ mol/dm^3. For the −12:+3 electrolyte the maximum of this distribution is at 4, which corresponds to a fully neutralized macroion. For the −12:+1 electrolyte and the

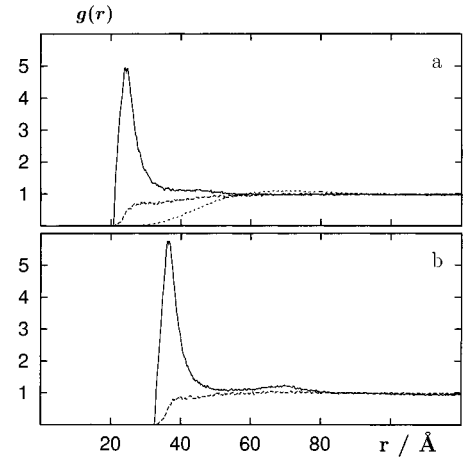

Figure 4. Molecular dynamics macroion−macroion pdfs for (a) −12:+1 (dotted), −12:+2 (dashed), and −12:+3 electrolyte (solid line) and (b) for −24:+2 (dashed) and −24:+3 electrolyte (solid line) all at the macroion concentration of 0.005 mol/dm^3.

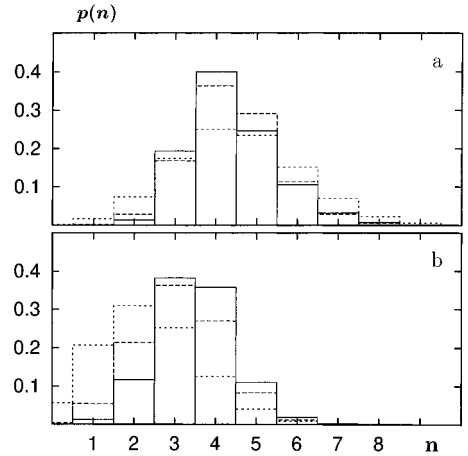

Figure 5. Distribution of the number of counterions in a macroion shell for −12:+1 (short dashes), −12:+2 (long dashes), and −12:+3 electrolyte (solid line) at a macroion concentration of 0.005 mol/dm^3. Data apply to two different cutoff values: $r_c = 20$ Å (a) and $r_c = 15$ Å (b).

−12:+2 electrolyte, the maxima are also found to be around 4. In these cases, however, the macroion (plus related counterions) has a net negative charge, since 12 monovalent or 6 divalent counterions are needed to neutralize any given macroion. Actually, no fully neutralized macroions were observed for the −12:+1 electrolyte under these conditions and only a few for the −12:+2 case. It is quite obvious from these results that the tendency of macroions to form clusters is closely associated with the ability of counterions to neutralize the macroion. Figure 5b shows the same distributions for a smaller cutoff value, i.e., for $r_c = 15$ Å. Obviously, the N_c distributions are shifted toward smaller numbers of counterions, but the basic features are the same as before. At the lower electrolyte concentration (c_m = 0.001 mol/dm^3) the trends are similar but the average number of counterions is slightly lower than for $c_m = 0.005$ mol/dm^3 for all counterion charges.

In the next step, we may define two macroions as bonded when they have at least one common counterion in their shell. We then define a cluster of macroions as the connected set of macroions bonded directly or indirectly (via an another macroion) to each other. Figure 6 shows on a logarithmic scale the probability distribution of the number of macroions in the clusters (as defined above) for the three different counterion

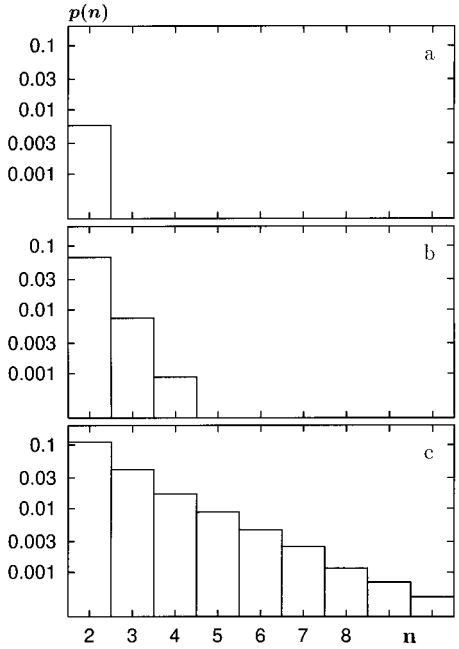

Figure 6. Size-of-cluster distribution for −12:+1 (a), −12:+2 (b), and −12:+3 electrolyte (c); $r_c = 20$ Å, and $c_m = 0.005$ mol/dm^3.

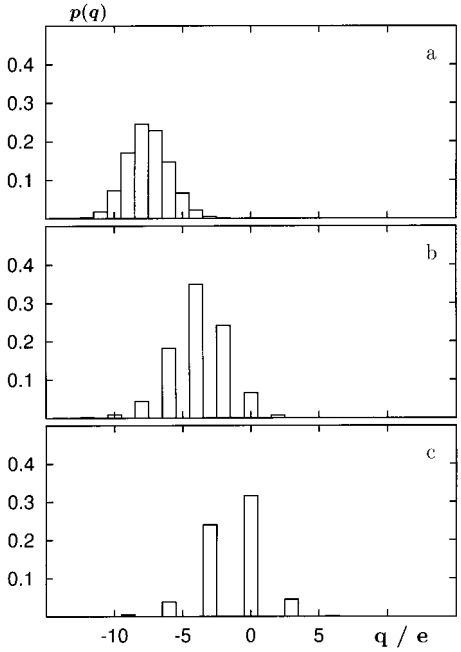

Figure 7. Charge-of-cluster distribution, notations as for Figure 6.

valencies at $c_m = 0.005$ mol/dm^3. In all cases the maximum of the distribution corresponds to isolated macroions (which is not shown here). For the −12:+2 electrolyte few macroion pairs (clusters consisting of 2 macroions) and even very few clusters with 3 or 4 macroions are observed. In the −12:+3 case more pairs and also larger clusters of up to 10 macroions are formed (however, with very low probability), which leads to the formation of a second maximum in the macroion−macroion distribution in Figure 4. Clearly, the change in the distribution of cluster size with increasing counterion charge is consistent with the observation of an increasing maximum in the macroion−macroion pdf.

In Figure 7 the probability distribution of total cluster charge is shown for the same three cases. The total cluster charge is defined as the sum of the macroion and counterion charges in the cluster. For solutions with monovalent counterions (−12:+1), where no clusters are formed, this distribution is essentially the same as the distribution of the number of counterions in the counterion shell (Figure 5), shifted by the macroion charge (−12e). The most probable cluster charge for clusters containing divalent counterions is −4e and only a few neutral clusters are observed. In contrast, in the case of trivalent counterions the distribution of the cluster charge peaks for neutral (net charge is zero) clusters.

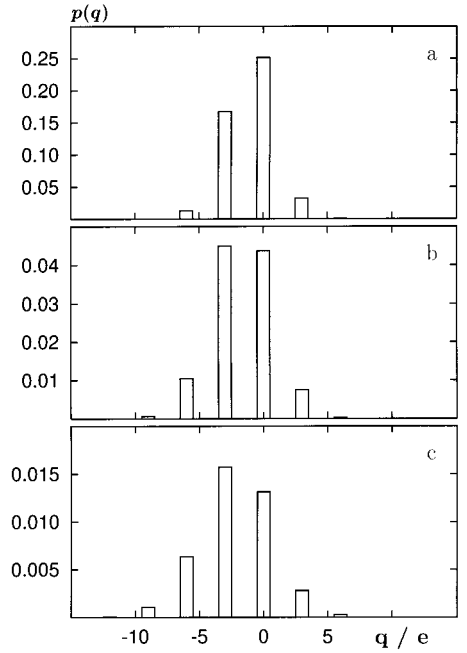

Figure 8. One-macroion (a), two-macroion (b), and three-macroion-cluster (c) charge distribution for a −12:+3 electrolyte, $c_m = 0.005$ mol/dm^3.

We can go one step further in our analysis and consider the charge distribution of various cluster types; monomers (Figure 8a), dimers (two macroions in a cluster; Figure 8b), and trimers (three macroions; Figure 8c) in the −12:+3 electrolyte. The monomers and the pair and triplet clusters are the predominant "species" in the solution. Isolated macroions are most likely to be fully neutralized by counterions or may have a residual charge of $-3e$. Few positive (overcharged) macroions exist. The probability of neutral and 3-fold negative macroion dimers is approximately the same, and again few positive clusters occur. This behavior is consistent with the following interpretation: Most macroion pairs are formed either by combining 2 neutral species or one neutral and one 3-fold negative species. Neutral and positive species, or negative and positive species, can also combine to form a pair of macroions but do not contribute much to the total. A similar argument holds for the formation of the much less frequent triplet clusters.

3.3. Dynamic Properties. From the MD results several dynamic properties can be analyzed. Here we limit our analysis to diffusion coefficients of the macroions and counterions and to lifetimes of various clusters in the solution. It should be noted that these properties depend to some extent on the chosen masses. More precisely, the absolute values of the diffusion coefficient depend on the masses; however, the trends and ratios provide meaningful insights into processes in the electrolyte solution.

Table 2 summarizes the diffusion coefficients as calculated from the mean square displacements of ions via the Einstein relation for some of the studied systems. We note that at both

TABLE 2: Self-Diffusion Coefficients D_i ($cm^2\ s^{-1}$)

	0.001 mol/dm^3		0.005 mol/dm^3	
	12:1	12:3	12:1	12:3
macroion (D_m)	0.0039	0.0360	0.0017	0.0070
counterion (D_c)	0.0455	0.0320	0.0097	0.0067
ratio D_m/D_c	0.09	1.13	0.18	1.05

TABLE 3: Residence Times (ps) As Defined in the Text for the Simulations of Macroions with Charge −12e at c_m = 0.005 mol/dm^3

counterion valency	τ_c	τ_{free}	$\tau_{cluster}$
+1	43	332	3
+2	95	58	9
+3	98	45	45

concentrations the monovalent counterions are substantially more mobile than the larger macroions. The self-diffusion coefficients of the counterions are 5−10 times larger than those of the macroions. In contrast, solutions containing trivalent ions exhibit similar diffusion coefficients for both species, indicated by the ratio D_m/D_c being around 1. Obviously, the trivalent ions are slowed due to the formation of neutralizing shells and clusters. We further note that self-diffusion coefficients decrease with increasing concentration, as expected.

In the cluster analysis above we defined the counterion shell around a given macroion as all those counterions that are within 20 Å from the macroion. We can calculate the residence time τ_c of a counterion in the shell of any macroion in a straightforward manner. Similarly, we can calculate the residence time $\tau_{cluster}$ of a macroion inside a macroion cluster (containing 2 or more macroions). Finally, we can calculate the average time that a macroion spends between leaving a cluster and becoming a member of the same or of another cluster, τ_{free}. We summarize these residence times for the macroions of charge −12e and for c_m = 0.005 mol/dm^3 in Table 3. In line with expectations based on the cluster size distribution, the lifetime of a free macroion τ_{free} decreases with increasing counterion charge (and increasing cluster formation), whereas the residence time of a macroion $\tau_{cluster}$ in the cluster increases along the same direction. In the case of trivalent counterions both lifetimes become approximately the same, consistent with the more extensive cluster formation observed under these conditions.

Finally, we note that in the cluster forming solutions (−12:+3 and −12:+2) the residence time of counterions in the macroion shell is substantially larger than the cluster residence times and the lifetimes of free macroions. This indicates that there are almost no free counterions in the solution and that the macroion−counterion "bond" is more stable than the macroion−macroion "bond". This can also be seen from snapshots (not shown here) and animations of the MD calculation.

4. Discussion

From the analysis of cluster structures and dynamics the following picture emerges: With increasing counterion charge, the ability of counterions to neutralize a macroion increases. In the −12:+1 solution no neutralized macroions exist and no cluster formation is observed. In the −12:+3 solution a large fraction of neutralized macroions exists and cluster formation is substantial. The −12:+2 solution is an intermediate case. The residence times indicate that the macroion−counterion "bonds" are more stable than the macroion−macroion "bonds".

We can thus cast this interpretation for the trivalent counterion case into quasi-chemical equilibrium in the following way: First, neutral or almost neutral precursors are formed out of a single macroion and counterions

$$m^{12-} + 4c^{3+} \rightleftharpoons mc_4^0\, K_1 \tag{2}$$

$$m^{12-} + 3c^{3+} \rightleftharpoons mc_3^{3-}\, K'_1 \tag{3}$$

where K_1 and K_1' are approximately equal, according to Figure 8. The fact that the counterion residence times are always larger than the cluster residence times justifies this precursor interpretation. In analogous equations for the monovalent case, K_1 would be much smaller (in fact, no neutral macroions are observed). As a consequence, the precursor cannot form. This, in turn, prevents the formation of dimers and higher clusters.

The precursors may combine to form dimers

$$mc_4 + mc_3^{3-} \rightleftharpoons m_2c_7^{3-}\, K_2 \tag{4}$$

and

$$mc_4 + mc_4 \rightleftharpoons m_2c_8^0 K_2' \tag{5}$$

Figure 8 indicates that K_2 and K_2' are approximately the same. Analogous equilibria for divalent and monovalent counterions are shifted to the left, indicating that the equilibrium constant K_2 is much smaller in the latter cases.

We performed a similar analysis for solutions of larger macroions with a higher charge (−24 e) and for divalent and trivalent counterions (parameter set II in Table 1). The macroion surface charge density in this case is about 16% smaller than for parameter set I. Again, we observe substantial cluster formation for trivalent counterions, but almost no macroion clusters are found in solutions with divalent counterions. Some exploratory studies at even higher macroion surface charge density lead, in agreement with previous studies,[24,30] to complete coagulation of the system when multivalent counterions are present. Thus, the surface charge density on the macroions is an important parameter driving cluster formation.[24,30]

In summary, our molecular dynamics simulations indicate that the formation of clusters between like-charged macroions requires the existence of neutralized or almost neutralized macroions as precursors. In solutions with monovalent counterions the formation of these neutralized precursors is highly unlikely. These conclusions are in close agreement with the results of a systematic study of a polyelectrolyte system with point counterions performed by Linse and Reščič.[24,30] These authors demonstrated that at high electrostatic coupling the counterions accumulate near the macroions and partially neutralize them. In view of our results presented above, this is a necessary condition for a macroion cluster formation. The parameters that control the electrostatic coupling are (i) the charge on macroions, (ii) dielectric permittivity (or/and temperature), and (iii) the counterion charge. Linse and Reščič[24,30] demonstrated that the system separates into two phases of different electrolyte concentration by increasing either the macroion or counterion charge and/or by decreasing the dielectric permittivity. Note that all three conditions (i−iii) yield a high accumulation of counterions near macroions; however, an increase of the counterion charge seems to be most effective in this process and consequently also in cluster formation.

After this paper was ready for submission, an important article of Jardat et al.[32] became available to us. These authors applied the Brownian dynamics (BD) simulation method to study aqueous solutions of −10:+1, −10:+2, and −20:+2 electrolytes with an asymmetry in size 2:15. The systems with these parameters were previously studied by the Monte Carlo method

and various integral equation techniques.[36,37] The BD results for the excess internal energy and pressure agree very well with the previously obtained MC data.[36,37] Jardat et al. performed a somewhat similar analysis of the counterion−macroion association as given in this paper. They found that the average number of counterions "condensed on macroions" at distances lower than the minimum of the macroion−macroion pdf increases with increasing electrolyte concentration, an observation analogous to ours. Some other conclusions arrived at in the BD study[32] are also consistent with our results. In particular they calculated the self-diffusion coefficients (actually $D/D°$, where $D°$ is the value at infinite dilution) of both ionic species as a function of the electrolyte concentration. Using their data, we calculated the ratio of the diffusion coefficients of macroions and counterions, D_m/D_c. Their result for a −10:+1 electrolyte at $c_m = 0.004\,98$ mol/dm^3 is $D_m/D_c = 0.091$, while our calculation for a −12:+1 solution at $c_m = 0.005$ mol/dm^3 (cf Table 2) gives $D_m/D_c = 0.18$. Unfortunately, Jardat et al.[32] do not provide any data for solutions with trivalent counterions. In conclusion, the molecular dynamics calculation of highly asymmetric electrolyte solutions presented here yields results consistent with recent Monte Carlo[19,30] and Brownian dynamics studies.[32]

Acknowledgment. This work was supported by the Slovene Ministry of Science and Technology (505). E.S. thanks the Faculty of Chemistry and Chemical Technology, of the University of Ljubljana, for its hospitality. V.V. acknowledges stimulating discussions with Professor Per Linse.

References and Notes

(1) Deryaguin, B. V.; Landau, L. *Acta Phys. Chem. USSR* **1941**, *14*, 633.
(2) Verwey, E. J. W.; Overbeek, J. Th. G. *Theory of the Stability of Lyophobic Colloids*; Elsevier: New York, 1948.
(3) Schmitz, K. S. *Macroions in Solution and Colloidal Suspension*; VCH: New York, 1992.
(4) Vlachy, V. *Annu. Rev. Phys. Chem.* **1999**, *50*, 145.
(5) Hansen J. P.; Lowen, H. *Annu. Rev. Phys. Chem.* **2000**, *51*, 209.
(6) Belloni, L. *J. Phys. Conds. Matter*, **2000**, *12*, R549.
(7) Bhuiyan, B.; Vlachy, V.; Outhwaite, C. *Int. Rev. Phys. Chem.* **2002**, *21*, 1.
(8) Gosule, L. C.; Schellman, J. A. *Nature* **1976**, *259*, 333.
(9) Bloomfield, V. A. *Biopolymers* **1997**, *44*, 269.
(10) Tang, J. X.; Wong, S.; Tran, P. T.; Janmey, P. A. *Ber. Bunsen-Ges. Phys. Chem.* **1996**, *100*, 796.
(11) Koltover, I.; Wagner, K.; Safinya, C. R. *Proc. Natl. Acad. Sci. U.S.A.* **2000**, *97*, 14046.
(12) Gröhn, F.; Antonietti, M. *Macromolecules* **2000**, *33*, 5938.
(13) Hribar, B.; Vlachy, V. *J. Phys. Chem. B* **1997**, *101*, 3457.
(14) Wu, J.; Bratko, D.; Prausnitz, J. M. *Proc. Natl. Acad. Sci. U.S.A.* **1998**, *95*, 15169.
(15) Allahyarov, E.; D'Amico, I.; Löwen, H. *Phys. Rev. Lett.* **1998**, *81*, 1334.
(16) Linse, P.; Lobaskin, V. *Phys. Rev. Lett.* **1999**, *83*, 4208.
(17) Schmidt A. B. *J. Chem. Phys.* **1999**, *265*, 432.
(18) Levine Y. *Physica A* **1999**, *110*, 1313.
(19) Hribar, B.; Vlachy, V. *Biophys. J.* **2000**, *78*, 694.
(20) Hribar, B.; Vlachy, V. *J. Phys. Chem. B* **2000**, *104*, 4218.
(21) Hribar, B.; Vlachy, V. *Rev. Soc. Quim. Mex.* **2000**, *44*, 11.
(22) Hribar, B.; Vlachy, V. *Acta Chim. Slov.* **2000**, *47*, 123.
(23) Linse, P.; Lobaskin, V. *J. Chem. Phys.* **2000**, *112*, 3917.
(24) Linse, P. *J. Chem. Phys.* **2000**, *113*, 1.
(25) Messina, R.; Holm, C.; Kremer, K. *Phys. Rev. Lett.* **2000**, *85*, 872.
(26) Messina, R.; Holm, C.; Kremer, K. *Europhys. Lett.* **2000**, *51*, 461.
(27) Trizac, R. *Phys. Rev. E* **2000** *62*, R1465.
(28) Delville, A.; Pellenq, R. J. M. *Mol. Simul.* **2000**, *24*, 1.
(29) Hribar, B.; Vlachy, V. *Langmuir* **2001**, *17*, 2043.
(30) Reščič, J.; Linse, P. *J. Chem. Phys.* **2001**, *114*, 10131.
(31) Lobaskin, V.; Lyubartsev, A.; Linse, P. *Phys. Rev. E* **2001**, *63*, R401.
(32) Jardat, M.; Cartailler, T.; Turq, P. *J. Chem. Phys.* **2001**, *115*, 1066.
(33) Henderson, D.; Duh, D.-M.; Chu, X.; Wasan, D. *J. Colloid Interface Sci.* **1997**, *185*, 265.
(34) Berendsen, H. J. C.; Postma, J. P. M.; van Gunsteren, W. F.; DiNola, A.; Haak, J. R. *J. Chem. Phys.* **1984**, *81*, 3684.
(35) Allen, M. P.; Tildesley, D. J. *Computer simulations of liquids*; Oxford University: New York, 1989.
(36) Hribar, B.; Kalyuzhnyi, Yu. V.; Vlachy, V. *Mol. Phys.* **1996**, *87*, 1317.
(37) Lobaskin, V.; Linse, P. *J. Chem. Phys.* **1998**, *109*, 3530.